The Structure of Murine Neuroglobin: Novel Pathways for Ligand Migration and Binding

Beatrice Vallone,[1]* Karin Nienhaus,[2] Maurizio Brunori[1] and G. Ulrich Nienhaus[2,3]*
[1]*Department of Biochemical Sciences, University of Rome "La Sapienza," Rome, Italy*
[2]*Department of Biophysics, University of Ulm, Ulm, Germany*
[3]*Department of Physics, University of Illinois at Urbana-Champaign, Urbana, Illinois*

ABSTRACT **Neuroglobin, a recently discovered globin predominantly expressed in neuronal tissue of vertebrates, binds small, gaseous ligands at the sixth coordination position of the heme iron. In the absence of an exogenous ligand, the distal histidine (His64) binds to the heme iron in the ferrous and ferric states. The crystal structure of murine ferric (met) neuroglobin at 1.5 Å reveals interesting features relevant to the ligand binding mechanism. Only weak selectivity is observed for the two possible heme orientations, the occupancy ratio being 70:30. Two small internal cavities are present on the heme distal side, which enable the His64(E7) side chain to move out of the way upon exogenous ligand binding. Moreover, a third, huge cavity (volume approximately 290 Å^3) connecting both sides of the heme, is open towards the exterior and provides a potential passageway for ligands. The CD and EF corners exhibit substantial flexibility, which may assist ligands in entering the protein and accessing the active site. Based on this high-resolution structure, further structure-function studies can be planned to elucidate the role of neuroglobin in physiological responses to hypoxia. Proteins 2004; 56:85–92.** © 2004 Wiley-Liss, Inc.

INTRODUCTION

Hemoglobin (Hb) and myoglobin (Mb) are classical representatives of the globins, an extended family of heme proteins that bind, transport, scavenge, detoxify, and sense small gaseous molecules such as O_2, NO, and CO.[1–7] The last years have witnessed the discovery of new globins in all kingdoms of life.[8–11] Neuroglobin (Ngb) is a recently discovered globin that is predominantly expressed in the brain and other nerve tissue of vertebrates.[12] Phylogenetic analysis revealed that Ngb forms a class distinct from the Mbs and Hbs, suggesting that this ancient protein existed long before the genes encoding Mb and Hb diverged.[12] The closest relatives of Ngb are the globins of the polychaete annelid worm *Aphrodite aculeata* (30% amino acid identity),[13] which are also expressed in nerve cells of this animal. The physiological function of Ngb is still a mystery. Its moderate affinity for O_2 (1–2 torr) and its expression in cerebral neurons suggest a role in neuronal responses to hypoxia or ischemia, as supported by several pieces of evidence, including recent experiments carried out in vivo.[14]

Ngb, a single polypeptide of 151 amino acids, bears only small sequence similarity to the vertebrate globins Mb (< 21%) and Hb (< 25%). Nevertheless, all key determinants of genuine globins[15] are conserved: a proximal histidine residue His96(F8) links the polypeptide chain to the heme iron, a distal histidine residue His64(E7) resides close to the binding site of the diatomic ligand, and a phenylalanine residue Phe42(CD1) is involved in π–π stacking interactions with the heme.[16] [In this paper, we quote the topological positions in parenthesis, according to the alignment with sperm whale (sw) Mb.]

Ngb is the first example of a vertebrate globin that is hexacoordinate in the "deoxy" ferrous form, in the absence of a bound exogenous ligand.[17–19] This feature was previously reported only for invertebrate[11,20] and plant globins.[21] Indeed, Ngb resembles nonsymbiotic plant hemoglobins[5,22,23]: (i) Key residues known to control the affinity for exogenous ligands (at positions B10, E7, and E11) are identical in both groups, being Phe, His, and Val, respectively; (ii) Ngbs and nonsymbiotic plant Hbs show "usual" association and dissociation rate coefficients in spite of unusual heme coordination[24] and (iii) Ngbs and nonsymbiotic plant Hbs are both expressed at low (micromolar) concentrations.

In the vast majority of globins, the met (Fe^{3+}) state is hexacoordinate, with an exogenous ligand, for example H_2O or OH^-, at the sixth coordination, whereas the ferrous deoxy (Fe^{2+}) form is generally pentacoordinate. In Ngb, the distal His64(E7) is coordinated to the heme iron in both the ferrous and ferric forms; because of the absence of an exogenous ligand, they are conventionally referred to as "unliganded."

Grant sponsor: the Deutsche Forschungsgemeinschaft; Grant numbers: Ni-291/3 and SFB 569; Grant sponsor: the Italian Consiglio Nazionale delle Ricerche (CNR) (Progetto "Genomica Funzionale"); Grant sponsor: the Centro di Eccellenza in Biologia e Medicina Molecolare of the M.I.U.R. Grant sponsor: M.I.U.R. (Progetto F.I.R.B. 2001 RBAU015B47_005).

The first two authors contributed equally to this work.

*Correspondence to: Beatrice Vallone, Department of Biochemical Sciences and University of Rome "La Sapienza," P.le A. Moro 5, 00185 Rome, Italy. E-mail: beatrice.vallone@uniroma1.it or G. Ulrich Nienhaus,Department of Physics, University of Illinois at Urbana-Champaign, 1110 W. Green, Urbana, IL 61801. E-mail: uli@uiuc.edu

Received 3 September 2003; Accepted 17 December 2003

Published online 7 May 2004 in Wiley InterScience (www.interscience.wiley.com). DOI: 10.1002/prot.20113

The structure of Ngb must be predisposed to accommodate the exchange of the endogenous imidazole side chain of His64(E7) for the exogenous, gaseous ligand, which is considered a novel mechanism for regulating ligand binding affinity. This interesting dynamic process was studied spectroscopically in great detail,[18] and fluctuations between different conformations were observed on surprisingly long time scales. To elucidate the function and dynamics of Ngb, detailed knowledge of the high resolution three-dimensional structure of both oxidation states with and without bound exogenous ligands is a prerequisite.

In this work, we present a high-resolution structure (1.50 Å) of ferric murine Ngb. Recently, Pesce et al.[16] have reported the structure of ferric human Ngb (hNgb) at 1.95 Å resolution. As expected from the high sequence identity (94%), the overall structures of the two proteins are very similar, with the same hexacoordinate heme iron geometry and a large internal cavity. However, the significantly higher resolution of the murine Ngb structure allows us to clearly pinpoint and quantify the unique heterogeneity of heme insertion. Moreover, our structure reveals a connection of the large internal cavity with the bulk. Other features, evident at quasi-atomic resolution, such as a water molecule docked close to the distal His(E7), allow us to discuss in detail the structural rearrangements necessary to accommodate exogenous heme ligands.

These X-ray structures will help to clarify the physiological role of Ngb at the molecular level, which may offer new avenues to the therapy of stroke, since the expression level of Ngb correlates with the extent of ischemic brain damage.[14,25]

TABLE I. Summary of Crystallographic Analysis

Data collection statistics[a]		
Wavelength (Å)	1.7	1.2
Space group	R32	R32
a = b (Å)	87.42	86.97
c (Å)	111.44	110.82
Resolution range (Å)	20.0–1.90 (1.96–1.90)	20.0–1.50 (1.55–1.50)
Unique reflections	25084 (2387)	25971 (2563)
Completeness (%)	99.5 (95.1)	99.9 (100.0)
Redundancy	16.22 (9.33)	10.8 (7.0)
R_{merge}(overall)[b]	0.061 (0.24)	0.060 (0.536)
FOM	0.44	
FOM DM	0.65	
Refinement		
R_{cryst}		0.184
R_{free}		0.207
Number of protein atoms		1305
Number of waters		116
Rms deviation from ideality		
Bonds (Å)		0.015
Angles (°)		3.1
Average B-value (Å^2)[c]		
All atoms		40.9 (33.1)
Main chain		37.8 (28.7)
Heme		23.9
Side chains, water		43.2 (36.1)

[a]Numbers in parentheses refer to the highest resolution shell.
[b]$R_{merge} = \Sigma_{hkl} \Sigma_j \mid I_j(hkl) - \langle I(hkl)\rangle \mid / \Sigma_{hkl} \Sigma_j \langle I(hkl)\rangle$, with $I_j(hkl)$ representing the intensity of measurement j and $\langle I(hkl)\rangle$ the mean of measurements for the reflection hkl.
[c]Numbers in parentheses refer to average values calculated with disordered regions omitted.

MATERIALS AND METHODS

Crystallization

Murine Ngb (mutant C55S/C120S) was produced in *Escherichia coli* strain BL21(DE3)pLys as described.[18] This particular mutant was used since the presence of oxidizable cysteines in the wild type protein hindered crystallization. Crystals of murine neuroglobin mutant C55S/C120S were grown using the hanging-drop vapor-diffusion method. The Hampton research Crystal Screen I kit was used to screen for a large number of crystallization conditions. Each well contained 1 ml of buffer solution. Drops were prepared by mixing 5 μl of protein solution (10 mg protein dissolved in 1 ml of H_2O) and 5 μl of buffer solution. Plates were stored at 293°C. Crystallization occurred under two conditions: (i) 0.1 M HEPES-Na, pH 7.5, 1.5 M Li_2SO_4 and (ii) 0.1 M sodium acetate, pH 4.6, 2 M sodium formate.

Structure Determination

Crystals under condition (ii) reached a typical size of $0.15 \times 0.15 \times 0.15$ mm^3. They were subjected to X-ray data collection at the Elettra synchrotron source (Trieste, Italy), where they diffracted up to 1.5 Å resolution on a MAR CCD detector. The crystals belonged to space group R32, with cell parameters a = b = 86.97 Å, c = 110.82 Å, with one molecule in the asymmetric unit and a solvent content of 38.98%. Data were indexed and scaled using the programs Denzo and Scalepack.[26] Phasing was carried out by taking advantage of the presence of the iron atom in the heme prosthetic group.[27] A high redundancy data set was collected at a wavelength of 1.7 Å to maximize the Fe anomalous signal up to a resolution of 1.9 Å. A second data set was collected on the same crystal at λ = 1.2 Å at a resolution of 1.5 Å (see Table I). The anomalous data set was used for phase determination using the program Solve,[28] and the position of the iron atom was readily determined. Experimental phases were subsequently improved by use of the density modification protocol implemented in Resolve.[29] The experimental maps were readily interpretable; 120 amino acids (80%) of the total sequence and the heme were fitted into the initial electron density. Subsequent rounds of structural refinement and model building with Quanta (Accelrys, Inc.) and Refmac[30] led to tracing of most of the protein primary sequence (amino acids 3–150) and the addition of 116 water molecules (see Table I for model statistics). The geometry of the final model is excellent; 90.8% of the residues lie in the most favored regions of the Ramachandran plot, with 6.9% positioned in other allowed regions and only 2.3%, i.e., three residues, in generously allowed regions. Of these three residues, two (Asp81, Leu82) are located in a very mobile loop, and one (Asp149) is at the C terminus. The C and N termini as well as loops 41–51 and 77–85 are more

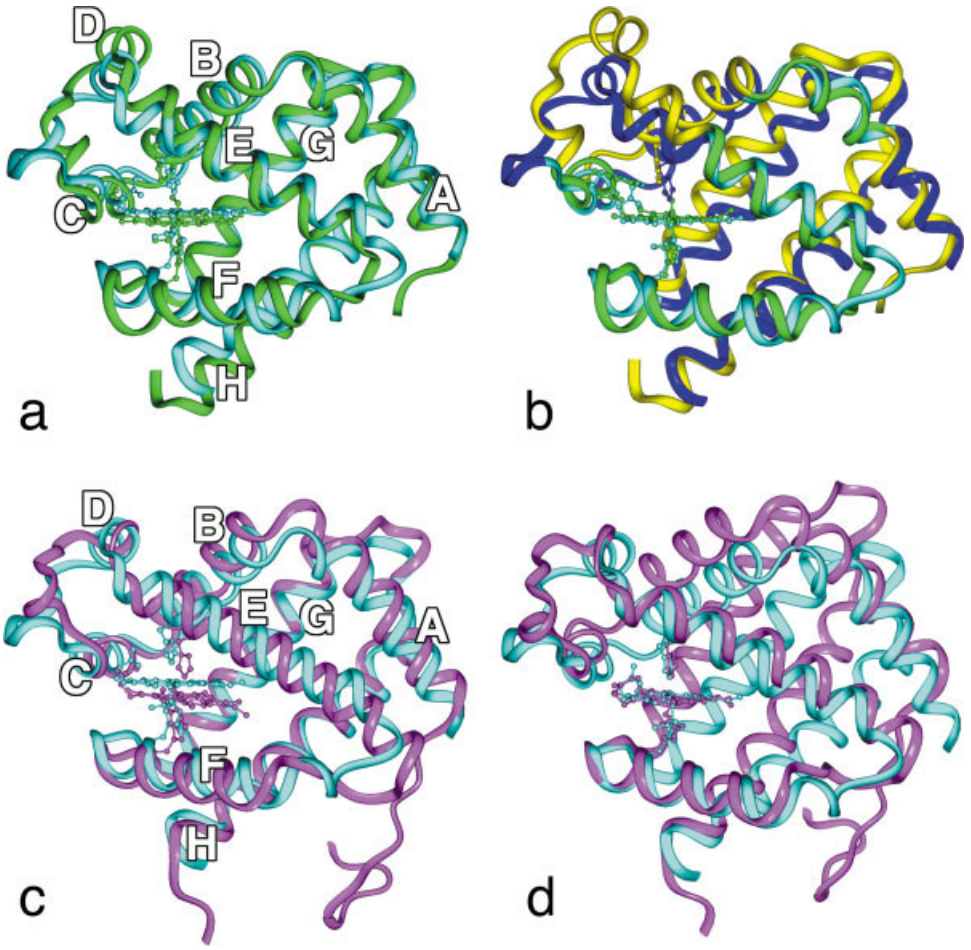

Fig. 1. Structural superposition of Ngb (light blue), swMb (green) and nsHb (pink). **a**: Best-fit superposition of Ngb and swMb, based on the C_α atoms. **b**: Best-fit superposition of Ngb and swMb, based on the porphyrin atoms. To emphasize the optimally superimposed main chain segments, less well superimposed segments are plotted in dark blue (Ngb) and yellow (swMb). **c**: Best-fit superposition of Ngb and nsHb, based on the C_α atoms. **d**: Best-fit superposition of Ngb and nsHb, based on the porphyrin atoms.

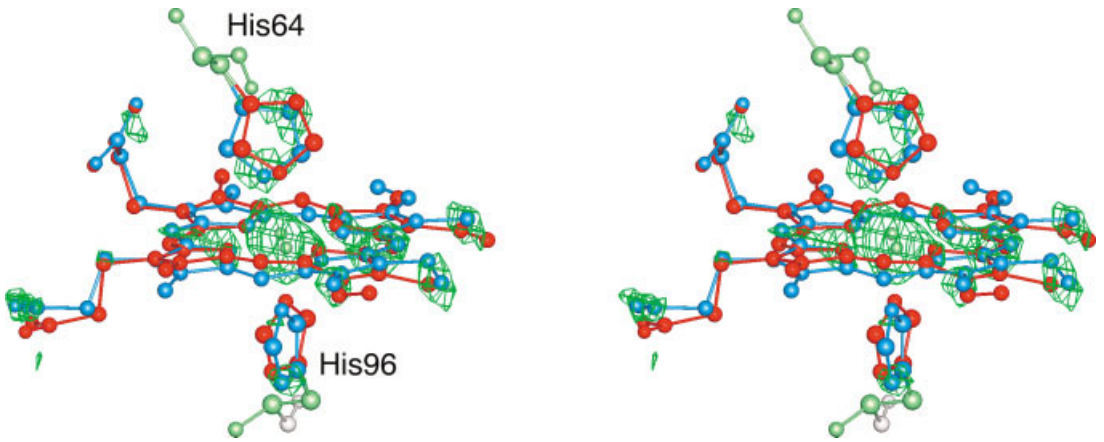

Fig. 2. Stereo view of the Fo–Fc positive electron density map calculated omitting the heme B conformer and the distal and proximal histidines of the B conformer. The A conformer had 70% occupancy. The density was contoured at 3 σ. The A (B) conformer is drawn in red (blue).

mobile than the rest of the structure and consequently show higher B-factors. Quality check on the structure was performed using PROCHECK,[30] data evaluation, transformation and refinement was carried out using programs from the CCP4 suite,[31] structure visualization was carried out using Quanta and InsightII (Accelrys, Inc.).

Cavity calculations and visualization were carried out using Surfnet[32].

The program defines gap regions by first filling the empty regions between atoms with gap-spheres. It then uses these to compute a 3D density map which, when contoured, defines the surface; the range used for gap spheres was 1.0–3.0 Å.

Structure factors and coordinates have been deposited with the Protein Data Bank in July 2003 and have the accession number 1Q1F.

RESULTS AND DISCUSSION

General Features of the Structure

The tertiary structure consists of 8 α-helices embedding the heme prosthetic group. The main helices are organized into a two-layer structure, recognized as a three-over-three α-helical sandwich.[16,33,34] The heme iron is hexacoordinated by four pyrrole N atoms within the heme plane, the distal histidine His64(E7) and the proximal histidine His96(F8). This geometry was clearly visible from the first electron density map produced after SAD phasing and density modification. A search in the Protein Data Bank for the closest structural relative using DALI[33] and CE[35] yielded in both cases sperm whale myoglobin (swMb, 2MGL and 1A6M), with the lowest root-mean-square deviation (RMSD) for C_α superposition of 2.00 Å and 15–17% identity in the structurally aligned sequences. We also carried out a structural superposition with rice non-symbiotic hemoglobin (nsHb, 1D8U) which yielded a comparable result, (RMSD = 2.24 Å, 17% identity) upon exclusion of the short N-terminal extension of nsHb. Therefore, despite its low sequence similarity (less that 25%) with vertebrate globins, Ngb clearly exhibits the architecture of this family.

Structural superposition of Ngb with swMb and nsHb by automatic alignment of C_α atoms is shown in Figure 1(a and c). If one superimposes the Ngb and nsHb structures using the porphyrin frame, it is apparent that the common feature of heme hexacoordination includes a similar arrangement of the rigid heme-helixE-helixF system,[36] including the orientation of His(E7) and His(F8) with respect to the heme atoms and the packing of the second half of the A helix onto helix F [Fig. 1(d)]. The other segments of Ngb and nsHb, however, are no longer optimally superimposed.

Superposition of Ngb and swMb by the porphyrin frame, however, slightly enhances the different geometries of the heme-helixE-helixF systems and still yields satisfactory alignment of the rest of the proteins [Fig. 1(b)]. In Ngb, the distal His64(E7) is shifted 2.38 Å closer to the heme iron with respect to pentacoordinated swMb. This shift can be ascribed to a rotation of the E helix around a pivot point at position Leu70(E13), for which the C_α positions are only 0.13 Å apart. This rotation separates the N and C tips of the E helices by 3.79 and 2.92 Å, respectively.

Structural Heterogeneity at the Binding Site

Given the close resemblance of Ngb with swMb, it was rather unexpected to find the main heme orientation within the Ngb protein moiety 180° rotated with respect to the α–γ meso axis. Even with this orientation, we still encountered difficulties in refining the heme iron position. Moreover, close inspection of the electron density maps revealed an expanded shape of the methyl groups in position 1 and 3, consistent with partial vinyl group occupancy. These findings suggested significant heterogeneity of the heme orientation, in agreement with recent solution NMR data by Du et al.[37] who reported heme orientational disorder for metNgb, with an approximately 2:1 predominance of the inverted geometry. By introducing a second, minor conformer (30% occupancy) in the "canonical" swMb insertion mode (Fig. 2) we could indeed refine the heme satisfactorily.

We have carefully analyzed the structure to identify the determinants of this unusual feature. Amino acids in close vicinity to the prosthetic group include Phe42(CD1), Leu92(F4), Val101(FG5), and Leu41(C7). There are no steric clashes with these residues in both heme orientations, and there is no obvious selectivity due to these residues. Phe42(CD1) is slightly disordered, as seen from its large B factors (Fig. 3). It also has a less well defined appearance in the electron density map. This residue is located at the border of the disordered CD loop, and reorganization of this loop may accompany ligand binding. In fact, the mobility of this region may be responsible for the low heme selectivity. Consistent with this hypothesis, Du et al.[37] reported a shift of the ratio of the two heme orientations from about 2:1 to about 1:1 upon cyanide binding. Another factor that reduces selectivity for a particular heme orientation is the lack of heme contacts at the methyl/vinyl B pyrrole side, opposite to the edge where Phe42(CD1) resides. This side of the heme provides some of the atoms that line a large cavity in Ngb, formed mainly by helices F and G. In swMb and nsHb, this cavity is reduced or absent.

In conjunction with the two heme conformations, the proximal His96(F8) and distal His64(E7) were also refined as two conformers, with the same 70:30 ratio of occupancies (Fig. 4). The reliability of the structural data is obviously higher for the dominant conformer A, which shows a more planar heme geometry, with a 0.20 Å out-of-plane displacement of the iron in the distal direction, similar to nsHb.[23] The iron position with respect to the heme plane is a major structural determinant of reactivity towards the ligand,[38] and a shift of the iron towards the distal side is consistent with the unexpected ligand affinity of Ngb.[39] The geometry of the His64(E7)N_ϵ-Fe-His96(F8)N_ϵ unit is nearly linear (177.3°), with distances of 1.9 and 2.2 Å between heme the iron and His64(E7) and His96(F8), respectively. By contrast, in conformer B, the iron is displaced by 0.27 Å towards the proximal side, and the angle defined by the two axial ligands and the iron is 156.0°; the distance between Fe and

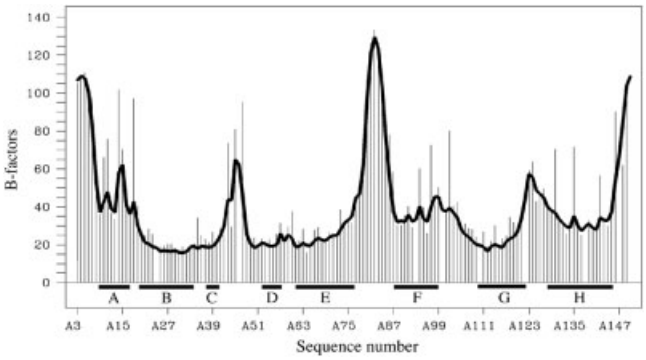

Fig. 3. Plot of thermal B-factors (in Å^2) versus mouse neuroglobin primary sequence position. The continuous line indicates the B-factors of the C_α atoms, the bars represent the average of side-chain B-factors.

His64(E7) is 2.1 Å, and the one between Fe and His96(E8) is 1.9 Å. The increased Fe-His64(E7) distance and the significantly distorted axial coordination may be consistent with less stable hexacoordination. Moreover, the different heme conformers support the heterogeneity observed in spectroscopic investigations.[17–19]

The distal pocket of Ngb, formed by residues Phe28(B10), Phe42(CD1) and Val68(E11), is hydrophobic in character except for His64(E7), the residue that prevents access of an exogenous ligand to the sixth coordination at the heme iron. Another functionally important residue is Lys67(E10). It is not unusual to find lysine or arginine at this position in the globin fold, as seen for example in *Aplysia limacina* Mb[40] and *Ascaris suum* Hb.[41] The long Lys67(E10) side chain presents a barrier to ligand exit and entry by forming a very stable salt bridge with one of the heme propionates (distance 2.7 Å), which is reinforced by a close contact to the hydroxyl group of Tyr44(CD3) and to a water molecule (Wat3 in Figure 4). Only upon disruption of this network can the distal histidine swing out of the distal pocket, an event which may cost up to 1.7 kcal/mol.[42,43] In the crystal lattice, there are additional interactions formed by the second heme propionate and Lys67(E10), due to contact with a symmetry-related protein molecule, which brings them to a distance of 2.7 Å (Lys67(E10)NZ-hemeO1A).

Hydrophobic Cavities in Ngb and Other Globins

The B factors of the C_α atoms and averages over the side-chain atoms are plotted in Figure 3. The core of the tertiary structure is well defined and covered by high-quality density structure, with the exception of a few residues at the C- and N-termini and the CD (41–51) and EF (77–85) corners. These two junctions between helical segments, though being continuous in the main chain electron density, posed problems in side-chain positioning (especially Asp81, Leu82, Ser83 and Ser84). Mobility of the CD corner was also observed in nsHb,[23] where it is probably correlated with rearrangements induced by ligand binding. In Ngb, there are short C and D helices that are absent in the plant protein; therefore, movements of the CD loop should be of lesser extent in Ngb. The marked mobility of the EF loop seen in Ngb (but absent in nsHb), seems to be correlated with a peculiar feature of Ngb, namely the presence of a large cavity at the heme side opposite to Phe42(CD1) which extends towards its distal side (Fig. 5), observed also in human Ngb.[16]

Internal cavities have been extensively studied in globins. We have calculated and compared the volumes of the cavities in the structures of Ngb, nsHb, and swMb, using the program Surfnet.[32] In swMb, structure analysis of crystals exposed to xenon revealed four cavities, a distal one (Xe4), two located at the heme rim (Xe2 and Xe3) and another on the proximal side (Xe1).[44] The volumes of Xe1-4 are 98.6, 70.0, 62.9 and 26.6 Å^3, respectively, as determined by Bossa et al. (manuscript in preparation). Recently, this cavity network has been studied extensively. Using site-directed mutagenesis or Xe to block migration pathways and fill the cavities, their role in ligand migration and binding was analyzed in detail.[45–50] It became apparent that these cavities play a crucial role in Mb, governing ligand dynamics and reactivity, because ligands transiently occupy these sites on their migration through the protein matrix. In nsHb we found only two cavities, located on the distal side of the heme, with volumes (62.4 Å^3 and 11.3 Å^3) smaller than the swMb distal side cavities. Ngb also displays two cavities on the distal side, a small apolar one, corresponding to Xe4 in Mb (15.9 Å^3) and an even smaller polar one (11.3 Å^3), which is in contact with the distal His64(E7) and hosts a water molecule (Wat9). The most interesting feature, however, is the presence of a third, huge cavity with a volume of 287.2 Å^3 (see Figure 5), corresponding to a fusion of the Xe2 and Xe1 cavities of swMb. This open volume connects the heme distal and proximal sides and has a highly hydrophobic character. This major "packing defect" is likely to be responsible for the lacking specificity for heme insertion in Ngb. More importantly, it may also be a crucial determinant for the function and dynamics of Ngb, because close inspection of the Xe1/2 cavity reveals a connection with the external surface of the protein through a channel flanked by Tyr88(F3). Although the orifice of this channel is fairly narrow in the crystal structure, it should allow easy access of diatomic ligands to the cavity, given the mobility of the EF corner that constitutes its "external wall." Similar channels have been detected in *Cerebratulus lacteus* hemoglobin[51] and *Mycobacterium tuberculosis* hemoglobin,[52] and their possible role in understanding the function of these proteins has been discussed.[51]

Modeling Exogenous Ligand Binding to Ngb

The presence of His64(E7) at the sixth coordination of the heme iron requires displacement of this side chain upon exogenous ligand binding [Fig. 6(a)]. Inspection of the distal side structure reveals two alternative modes to remove the endogenous imidazole ligand from the sixth coordination (Fig. 6): (1) it may either swing deeper into the distal pocket and dock in the cavity occupied by Wat9, or (2) it may swing out of the distal pocket, with concomitant breakage of the hydrogen bond

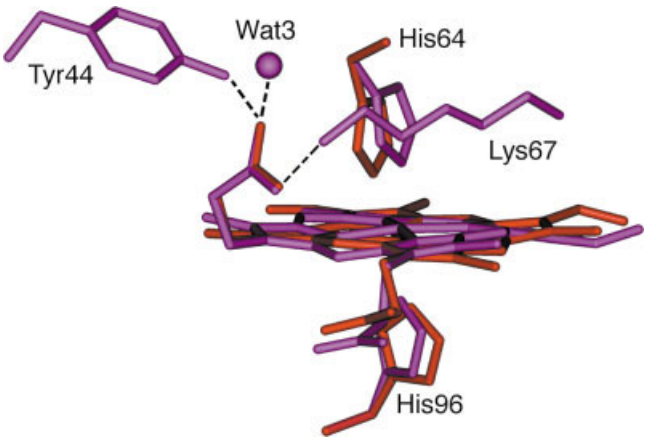

Fig. 4. The different heme conformers of Ngb. Blue: conformer A (70% occupancy). Red: conformer B (30%). Close distances are: Tyr44(CD3)—OH to heme propionate—O2A = 2.6 Å, heme propionate—O2A to Wat3 = 2.7 Å, Lys67(E10)—NZ to heme propionate—O1A = 2.7 Å.

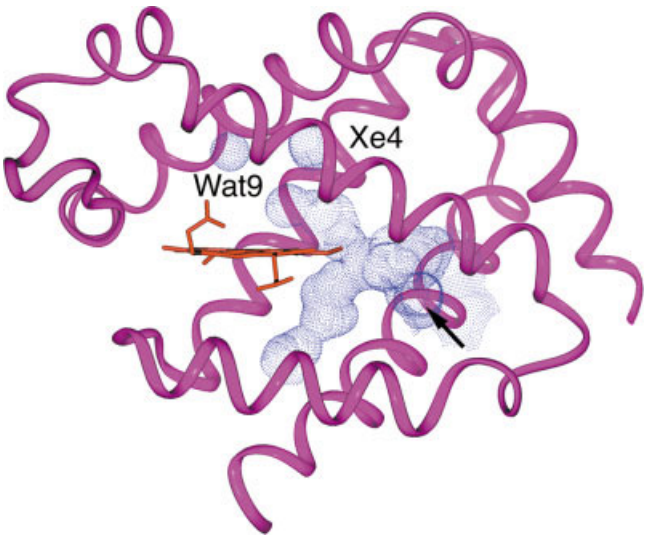

Fig. 5. Cavities in Ngb, as determined by using Surfnet.[32] Residues lining cavity Wat9: Phe28, Phe42, Phe61 and His64. Residues lining cavity Xe4: Gly24, Leu27, Ile65, Val68 and Met69. The residues lining the very large cavity are: Heme, Val71, Ile72, Ala74, Ala75, Leu85, Tyr88, Leu89, Leu103, Phe106, Val109, Leu113, Leu136, Tyr137, Val140, Val141, Met144, and Trp148. The arrow indicates the opening connecting the cavity with the bulk.

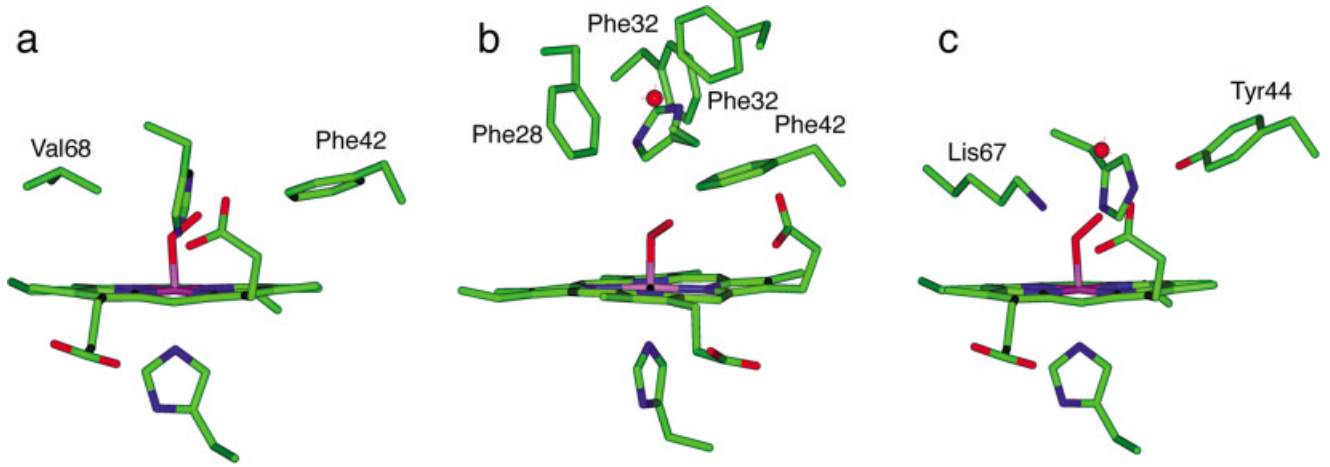

Fig. 6. Modeling dioxygen binding to the distal site of Ngb. **a**: The original His64(E7) position (χ_1 = 178.1°) overlaps with the first atom of the diatomic ligand (0.28 Å). **b**: His64(E7) swings towards the interior; at χ_1 = −72.5°, there are no close contacts of the imidazole side chain with other amino acids or with the bound ligand. **c**: His64(E7) swings towards the exterior; at χ_1 = 114.5°, there is a steric clash with O2A of the heme propionate (distance 0.63 Å) and close contact with Tyr44(CD3)-OH (2.14 Å) and Wat3 (1.95 Å).

network involving Tyr44(CD3), Lys67(E10), heme propionate and Wat3 (Fig. 4).

Figure 6(b) shows that rotation of the His64(E7) imidazole, by a change of the χ_1 angle from the experimentally determined value of 178.1° found in the met hexacoordinated state to 114.5°, is sufficient to almost entirely remove the overlap with the modeled ligand (introduced on the basis of the swMb oxy structure). This movement would necessitate expulsion of Wat9 from its cavity, but only modest rearrangements of the residues lining the cavity itself (Phe61(E3), Phe28(B10), and Phe42(CD1)); the latter two residues are two of the close heme contacts. Therefore, their reorientations would account for heme orientational disorder and rearrangement upon ligand binding.[37]

In the second mechanism, the distal histidine may swing towards the exterior [Fig. 6(c)]. This model was originally introduced for Mb[3] and later also invoked for other heme proteins.[53] In Ngb, changing the χ_1 angle of His64(E7) to −72.5° makes the distal pocket available for exogenous ligand binding. However, in this scenario, the imidazole side chain would collide with the heme propionate, Lys67(E10) and Tyr44(CD3), involved in the electrostatic/hydrogen bonding network depicted in Figure 4. Rearrangement of the mobile CD loop and sliding of the F helix, made possible by the mobile EF corner, could facilitate opening the way for the His64(E7) "swinging out" movement.

An infrared study of CO binding to ferrous Ngb provides clear evidence for these two mechanisms of His64(E7) move-

ment. Up to four CO stretching bands with pH-dependent amplitudes, known to arise from multiple His64(E7) conformers,[18] can be distinguished. At neutral and high pH, only two bands are visible, A_1 at 1940 cm^{-1} and A_2 at 1980 cm^{-1}. The frequency of the dominant A_1 conformer (~80%) is typical of globins, in which the His64(E7) imidazole places an imino hydrogen near the CO oxygen. In swMbCO, for example, the dominant conformer at neutral pH is characterized by an A_1 band at 1945 cm^{-1}. An additional shift to 1940 cm^{-1} is expected for NgbCO because of the presence of Phe28(B10). In MbCO, both Phe and Tyr replacements of Leu29(B10) cause a shift of the CO stretching band to lower frequency. The exceptionally high CO stretching frequency of the A_2 conformer in Ngb can be assigned to the imidazole tautomeric state, in which the proton sits on the other nitrogen. As a consequence, the lone-pair on the nitrogen would point towards the CO oxygen, causing an up-shift in frequency. These infrared observations provide clear evidence of mechanism 1 at physiological pH, in which the distal histidine moves deeper into the distal heme pocket upon ligand binding, as shown in Figure 6(b).

At low pH, two additional bands appear in the infrared spectrum of NgbCO; they are denoted as A_0 (1970 cm^{-1}) and A_3 (1925 cm^{-1}). By comparison with swMbCO, A_0 can be assigned to a conformation in which the distal histidine has swung out of the distal pocket, as described by our mechanism 2 [Fig. 6(c)]. This interpretation is supported by the observation that replacement of the imidazole by an aliphatic side chain in Ngb mutant His64(E7)L yields a single infrared band at 1971 cm^{-1} (Nienhaus et al., unpublished). As with the A_1 conformation, the low frequency of A_3 can be explained by the presence of a positive charge in the vicinity of the CO oxygen. But since the imidazole has swung out of the distal pocket after protonation, it cannot be responsible for this effect. Rather, we suggest that a water molecule enters the pocket and resides near the location of Wat9. Its hydrogen can then interact with the CO oxygen so as to shift its frequency.

In addition to the His64(E7) gate,[54] the tunnel to the large Xe1/2 pocket in the Ngb structure offers an alternate entry and exit route for ligands. In this case, swinging motion of the His64(E7) would follow ligand entry to enable binding rather than being a prerequisite for ligand access to the distal pocket.

CONCLUSIONS

The structure of mouse ferric (or met) Ngb at 1.5 Å resolution provides the structural framework necessary for unraveling its hitherto unresolved physiological function. Moreover, it allows one to correlate kinetic and spectroscopic data available on Ngb to its molecular properties. In the crystal structure, the heme is observed to be inserted into the protein in two different orientations, with an occupancy ratio of 70:30; the major conformer in Ngb is the species normally absent in native swMb. This characteristic was suggested but not systematically analyzed in the structure of hNgb,[16] possibly due to its lower resolution. The lack of orientational selectivity is possibly related to the presence of a very large cavity lining the heme and to the increased mobility of crucial heme contacts. Another significant source of heterogeneity, well documented kinetically and spectroscopically,[18,37] arises from multiple conformations of the imidazole side chain of His64(E7). Upon binding of an exogenous ligand, the imidazole is expected to move away from the sixth coordination by rotating either towards the interior or the exterior of the distal pocket. Mobility of the CD and EF corners also appears necessary to make the distal site available for ligation and enlarge the connection of the very large Xe1/2 cavity with the external medium. This cavity provides an entry and exit route for ligands; it can host photodissociated ligands in a vast, structurally diverse environment, in agreement with the complex dynamics observed in flash photolysis experiments.[18,55] Interestingly, it bifurcates at the level of the heme rim (Fig. 5) allowing access to both proximal and distal sides which raises the question whether proximal ligand binding might be possible, especially with nitric oxide.

The coexistence of diverse binding and access modes to the heme iron, the accessory entry path, and heme hexacoordination might constitute a sort of "molecular fossil" reminiscent of a redox catalytic function of the globin fold. Ngb might be involved in NO metabolism in the nervous tissue, which can become crucial in case of hypoxic events, as shown in vivo.[14] These data make Ngb a novel target for devising new strategies to minimize the effects of stroke. Our high-resolution structure of mouse Ngb may become crucial to achieve a detailed understanding of its functional role in the brain.

ACKNOWLEDGEMENTS

We thank Dr. C. Bossa and Dr. S. Della Longa for advice in computing protein cavities and heme parameters. Expert assistance by the Elettra staff scientists and F. Renzi during data collection is gratefully acknowledged. This work was supported by the Deutsche Forschungsgemeinschaft (Ni-291/3 and SFB 569 to G.U.N.), by the Italian Consiglio Nazionale delle Ricerche (CNR) to B.V. (Progetto "Genomica Funzionale"), by the Centro di Eccellenza in Biologia e Medicina Molecolare of the M.I.U.R., and by the M.I.U.R. Project RBAU015B47_005 to M.B.

REFERENCES

1. Perutz MF. Stereochemistry of cooperative effects in haemoglobin. Nature 1970;228:726–739.
2. Antonini E, Brunori, M. Hemoglobin and myoglobin in their reactions with ligands. Amsterdam: North-Holland, 1971.
3. Perutz MF. Myoglobin and haemoglobin: role of distal residues in reactions with haem ligands. Trends Biochem Sci. 1989;14:42–44.
4. Frauenfelder H, McMahon BH, Austin RH, Chu K, Groves JT. The role of structure, energy landscape, dynamics, and allostery in the enzymatic function of myoglobin. Proc Natl Acad Sci USA 2001;98: 2370–2374.
5. Pesce A, Bolognesi M, Bocedi A, Ascenzi P, Dewilde S, Moens L, Hankeln T, Burmester T. Neuroglobin and cytoglobin. Fresh blood for the vertebrate globin family. EMBO Rep. 2002;3:1146–1151.
6. Couture M, Yeh SR, Wittenberg BA, Wittenberg JB, Ouellet Y, Rousseau DL, Guertin M. A cooperative oxygen-binding hemoglobin from Mycobacterium tuberculosis. Proc Natl Acad Sci USA 1999;96:11223–11228.
7. Yeh SR, Couture M, Ouellet Y, Guertin M, Rousseau DL. A cooperative oxygen binding hemoglobin from Mycobacterium tuber-

culosis. Stabilization of heme ligands by a distal tyrosine residue. J Biol Chem 2000;275:1679–1684.
8. Hankeln T, Rozynek P, Schmidt ER. The nucleotide sequence and in situ localization of a gene for a dimeric haemoglobin from the midge Chironomus thummi piger. Gene 1988;64:297–304.
9. Gardner PR, Gardner AM, Martin LA, Salzman AL. Nitric oxide dioxygenase: an enzymic function for flavohemoglobin. Proc Natl Acad Sci USA 1998;95:10378–10383.
10. Potts M, Angeloni SV, Ebel RE, Bassam D. Myoglobin in a cyanobacterium. Science 1992;256:1690–1691.
11. Couture M, Das TK, Lee HC, Peisach J, Rousseau DL, Wittenberg BA, Wittenberg JB, Guertin M. Chlamydomonas chloroplast ferrous hemoglobin. Heme pocket structure and reactions with ligands. J Biol Chem 1999;274:6898–6910.
12. Burmester T, Weich B, Reinhardt S, Hankeln T. A vertebrate globin expressed in the brain. Nature 2000;407:520–523.
13. Dewilde S, Blaxter M, Van Hauwaert ML, Vanfleteren J, Esmans EL, Marden M, Griffon N, Moens L. Globin and globin gene structure of the nerve myoglobin of Aphrodite aculeata. J Biol Chem 1996;271:19865–19870.
14. Sun Y, Jin K, Peel A, Mao XO, Xie L, Greenberg DA. Neuroglobin protects the brain from experimental stroke in vivo. Proc Natl Acad Sci USA 2003;100:3497–3500.
15. Bashford D, Chothia C, Lesk AM. Determinants of a protein fold. Unique features of the globin amino acid sequences. J Mol Biol 1987;196:199–216.
16. Pesce A, Dewilde S, Nardini M, Moens L, Ascenzi P, Hankeln T, Burmester T, Bolognesi M. Human brain neuroglobin structure reveals a distinct mode of controlling oxygen affinity. Structure (Camb) 2003;11:1087–1095.
17. Couture M, Burmester T, Hankeln T, Rousseau DL. The heme environment of mouse neuroglobin. Evidence for the presence of two conformations of the heme pocket. J Biol Chem 2001;276: 36377–36382.
18. Kriegl JM, Bhattacharyya AJ, Nienhaus K, Deng P, Minkow O, Nienhaus GU. Ligand binding and protein dynamics in neuroglobin. Proc Natl Acad Sci USA 2002;99:7992–7997.
19. Trent JT, Watts RA, Hargrove MS. Human neuroglobin, a hexacoordinate hemoglobin that reversibly binds oxygen. J Biol Chem 2001;276:30106–30110.
20. Couture M, Das TK, Savard PY, Ouellet Y, Wittenberg JB, Wittenberg BA, Rousseau DL, Guertin M. Structural investigations of the hemoglobin of the cyanobacterium Synechocystis PCC6803 reveal a unique distal heme pocket. Eur J Biochem 2000;267:4770–4780.
21. Scott NL, Falzone CJ, Vuletich DA, Zhao J, Bryant DA, Lecomte JT. Truncated hemoglobin from the cyanobacterium Synechococcus sp. PCC 7002: evidence for hexacoordination and covalent adduct formation in the ferric recombinant protein. Biochemistry 2002;41:6902–6910.
22. Goodman MD, Hargrove MS. Quaternary structure of rice nonsymbiotic hemoglobin. J Biol Chem 2001;276:6834–6839.
23. Hargrove MS, Brucker EA, Stec B, Sarath G, Arredondo-Peter R, Klucas RV, Olson JS, Phillips GN, Jr. Crystal structure of a nonsymbiotic plant hemoglobin. Structure Fold Des 2000;8:1005–1014.
24. Arrendondo-Peter R, Hargrove MS, Sarath G, Moran JF, Lohrman J, Olson JS, Klucas RV. Rice hemoglobins. Gene cloning, analysis, and O2-binding kinetics of a recombinant protein synthesized in Escherichia coli. Plant Physiol 1997;115:1259–1266.
25. Sun Y, Jin K, Mao XO, Zhu Y, Greenberg DA. Neuroglobin is up-regulated by and protects neurons from hypoxic-ischemic injury. Proc Natl Acad Sci USA 2001;98:15306–15311.
26. Otwinowski Z, Minor W. Processing X-ray diffraction data collected in oscillation mode. Methods Enzymol 1996;276:307–326.
27. Dauter Z, Dauter M, Dodson E. Jolly SAD. Acta Crystallogr D Biol Crystallogr 2002;58:494–506.
28. Terwilliger TC, Berendzen J. Automated MAD and MIR structure solution. Acta Crystallogr D Biol Crystallogr 1999;55:849–861.
29. Terwilliger TC. Maximum-likelihood density modification. Acta Crystallogr D Biol Crystallogr 2000;56:965–972.
30. Laskowski RA, Macarthur MW, Moss DS, Thornton JM. Procheck—a program to check the stereochemical quality of protein structures. J Appl Crystallogr 1993;26:283–291.
31. CCP4. The CCP4 suite: programs for protein crystallography. Acta Crystallogr D Biol Crystallogr 1994;50:760–763.
32. Laskowski RA. SURFNET: a program for visualizing molecular surfaces, cavities, and intermolecular interactions. J Mol Graph 1995;13:323–330.
33. Holm L, Sander C. Protein folds and families: sequence and structure alignments. Nucleic Acids Res 1999;27:244–247.
34. Holm L, Ouzounis C, Sander C, Tuparev G, Vriend G. A database of protein structure families with common folding motifs. Protein Sci 1992;1:1691–1998.
35. Shindyalov IN, Bourne PE. Protein structure alignment by incremental combinatorial extension (CE) of the optimal path. Protein Eng 1998;11:739–747.
36. Kachalova GS, Popov AN, Bartunik HD. A steric mechanism for inhibition of CO binding to heme proteins. Science 1999;284:473–476.
37. Du W, Syvitski R, Dewilde S, Moens L, La Mar GN. Solution (1)h NMR characterization of equilibrium heme orientational disorder with functional consequences in mouse neuroglobin. J Am Chem Soc 2003;125:8080–8081.
38. Ormos P, Szaraz S, Cupane A, Nienhaus GU. Structural factors controlling ligand binding to myoglobin: a kinetic hole-burning study. Proc Natl Acad Sci USA 1998;95:6762–6767.
39. Liong EC, Dou Y, Scott EE, Olson JS, Phillips GN, Jr. Waterproofing the heme pocket. Role of proximal amino acid side chains in preventing hemin loss from myoglobin. J Biol Chem 2001;276: 9093–9100.
40. Conti E, Moser C, Rizzi M, Mattevi A, Lionetti C, Coda A, Ascenzi P, Brunori M, Bolognesi M. X-ray crystal structure of ferric Aplysia limacina myoglobin in different liganded states. J Mol Biol 1993;233:498–508.
41. De Baere I, Perutz MF, Kiger L, Marden MC, Poyart C. Formation of two hydrogen bonds from the globin to the heme-linked oxygen molecule in Ascaris hemoglobin. Proc Natl Acad Sci USA 1994;91: 1594–1597.
42. Horovitz A, Serrano L, Avron B, Bycroft M, Fersht A R, Strength and cooperativity of contributions of surface salt bridges to protein stability. J Mol Biol 1990;216:1031–1044.
43. Takano K, Tsuchimori K, Yamagata Y, Yutani K, Contribution of salt bridges near the surface of a protein to the conformational stability. Biochemistry 2000;39:12375–12381.
44. Tilton RF, Jr., Kuntz ID, Jr., Petsko GA. Cavities in proteins: structure of a metmyoglobin-xenon complex solved to 1.9 Å. Biochemistry 1984;23:2849–2857.
45. Nienhaus K, Deng P, Kriegl JM, Nienhaus GU. Structural dynamics of myoglobin: the effect of internal cavities on ligand migration and binding. Biochemistry 2003;42:9647–9658.
46. Nienhaus K, Deng P, Kriegl JM, Nienhaus GU. Structural dynamics of myoglobin: spectroscopic and structural characterization of ligand docking sites in myoglobin mutant L29W. Biochemistry 2003;42:9633–9646.
47. Scott EE, Gibson QH, Olson JS. Mapping the pathways for O2 entry into and exit from myoglobin. J Biol Chem 2001;276:5177–5188.
48. Brunori M, Gibson QH. Cavities and packing defects in the structural dynamics of myoglobin. EMBO Rep 2001;2:674–679.
49. Ostermann A, Waschipky R, Parak FG, Nienhaus GU. Ligand binding and conformational motions in myoglobin. Nature 2000; 404:205–208.
50. Bourgeois D, Vallone B, Schotte F, Arcovito A, Miele AE, Sciara G, Wulff M, Anfinrud P, Brunori M. Complex landscape of protein structural dynamics unveiled by nanosecond Laue crystallography. Proc Natl Acad Sci USA 2003;100:8704–8709.
51. Pesce A, Nardini M, Dewilde S, Ascenzi P, Riggs AF, Yamauchi K, Geuens E, Moens L, Bolognesi M. Crystallization and preliminary X-ray analysis of neural haemoglobin from the nemertean worm Cerebratulus lacteus. Acta Crystallogr D Biol Crystallogr 2001;57:1897–1899.
52. Milani M, Pesce A, Ouellet Y, Ascenzi P, Guertin M, Bolognesi M. Mycobacterium tuberculosis hemoglobin N displays a protein tunnel suited for O2 diffusion to the heme. EMBO J 2001;20:3902–3909.
53. Hargrove MS. A flash photolysis method to characterize hexacoordinate hemoglobin kinetics. Biophys J 2000;79:2733–2738.
54. Perutz MF, Mathews, F. S. An x-ray study of azide methaemoglobin. J Mol Biol 1966:21:199–202.
55. Van Doorslaer S, Dewilde S, Kiger L, Nistor SV, Goovaerts E, Marden MC, Moens L. Nitric oxide binding properties of neuroglobin. A characterization by EPR and flash photolysis. J Biol Chem 2003;278:4919–4925.
56. Lawson DM, Stevenson CE, Andrew CR, Eady RR. Unprecedented proximal binding of nitric oxide to heme: implications for guanylate cyclase. Embo J 2000;19:5661–5671.